sustainability

Article

Optimal Allocation of Energy Storage Capacity in Microgrids Considering the Uncertainty of Renewable Energy Generation

Wei Wei [1,*], Li Ye [1], Yi Fang [1], Yingchun Wang [1], Xi Chen [2,*] and Zhenhua Li [2,3]

[1] State Grid Hubei Marketing Service Center (Measurement Center), Wuhan 443080, China; yel16@163.com (L.Y.); xmwlelin@163.com (Y.F.); wangyc@126.com (Y.W.)
[2] College of Electrical Engineering and New Energy, China Three Gorges University, Yichang 443002, China; lizhenhua@ctgu.edu.cn
[3] Hubei Provincial Key Laboratory for Operation and Control of Cascaded Hydropower Station, China Three Gorges University, Yichang 443002, China
* Correspondence: sfdxlw@163.com (W.W.); 202108580021033@ctgu.edu.cn (X.C.)

Abstract: The high dimensionality and uncertainty of renewable energy generation restrict the ability of the microgrid to consume renewable energy. Therefore, it is necessary to fully consider the renewable energy generation of each day and time period in a long dispatching period during the deployment of energy storage in the microgrid. To this end, a typical multi-day scenario set is used as the simulation operation scenario, and an optimal allocation method of microgrid energy storage capacity considering the uncertainty of renewable energy generation is designed. Firstly, the historical scenarios are clustered into K types of daily state types using the K-means algorithm, and the corresponding probability distribution is obtained. Secondly, the Latin hypercube sampling method is used to obtain the state type of each day in a multi-day scenario set. Then, the daily scenario generation method based on conditional generative adversarial networks is used to generate a multi-day scenario set, combining the day state type as a condition, and then the typical scenario set is obtained using scenario reduction. Furthermore, a double-layer optimization allocation model for the energy storage capacity of microgrids is constructed, in which the upper layer optimizes the energy storage allocation capacity and the lower layer optimizes the operation plans of microgrids in each typical scenario. Finally, the proposed model is solved using the PSO algorithm nested with the CPLEX solver. In the microgrid example, the proposed method reduces the expected annual total cost by 19.66% compared with the stochastic optimal allocation method that assumes the scenic power obeys a specific distribution, proving that it can better cope with the uncertainty of renewable energy generation. At the same time, the expected annual total cost is reduced by 6.99% compared with the optimal allocation method that generates typical daily scenarios based on generative adversarial networks, which proves that it can better cope with the high dimensionality of renewable energy generation.

Keywords: uncertainty; optimize allocation; Latin hypercube sampling; conditional generation adversarial network

Citation: Wei, W.; Ye, L.; Fang, Y.; Wang, Y.; Chen, X.; Li, Z. Optimal Allocation of Energy Storage Capacity in Microgrids Considering the Uncertainty of Renewable Energy Generation. *Sustainability* **2023**, *15*, 9544. https://doi.org/10.3390/su15129544

Academic Editors: Wenlong Fu, Xun Shen and Nan Yang

Received: 17 May 2023
Revised: 4 June 2023
Accepted: 8 June 2023
Published: 14 June 2023

1. Introduction

In recent years, the permeability of distributed renewable energy power generation in microgrids has been increasing continuously [1,2], and the uncertainty of its output has increased the difficulty for microgrids to absorb renewable energy and operate reliably [3–6]. Appropriate allocation of energy storage equipment in microgrids is an effective means to deal with the uncertainty of renewable energy generation.

Allocating a reasonable amount of energy storage capacity to a microgrid can improve its operational economy and power supply reliability [7,8]. To obtain a reasonable capacity of energy storage configuration for microgrids, the literature [9] constructed an energy storage configuration model with minimizing the operation and investment cost, power loss cost, and CO_2 emission cost of energy storage as the economic and operational objectives, which successfully improved the economy of system operation. For the energy storage allocation problem of systems containing renewable energy, an optimization method that takes into account the uncertainty of new energy generation is necessary. A robust optimization method is an effective way to deal with uncertainty. In order to deal with the scenario of wind speed uncertainty, reference [10] established the distribution network operator's wind speed uncertainty set to represent its power generation range, so as to obtain the day-ahead robust optimal scheduling strategy of wind power and thermal power unit systems, so that the scheduling plan can be more flexible to deal with the uncertainty of renewable energy. In terms of energy storage capacity allocation, the robust optimization model of energy storage capacity allocation of distribution networks is established in reference [11]. However, the robust optimization needs to meet the adverse scenarios even under extremely low probabilities, which makes the scheduling scheme too conservative. Therefore, reference [12] proposes a planning method involving commitment and economic scheduling of hourly robust transmission constraint units, which can better evaluate operating costs under specific planning decisions and reduce the conservatism of robust optimization to a certain extent. To further reduce the conservatism of optimization results, reference [13] generates wind power generation scenarios based on Latin Hypercube Sampling (LHS) based on the renewable energy generation probability density distribution function, adopts the randomly optimized energy storage capacity allocation method, and takes the expected optimal under an uncertain environment as the goal. The flexibility and economy of the system are taken into account, but the probability density distribution function of renewable energy generation is often unknown in the actual planning work. In references [7,14], it is assumed that the wind power generation in the system conforms to the Weibull distribution and Gaussian distribution, respectively, and the wind power generation scenario set of renewable energy is obtained by sampling the wind power at each period to improve the adaptability of the optimal allocation results of energy storage to the uncertainties of wind power generation. However, in reality, the probability distribution of renewable energy generation power is often unknown, and assuming that renewable energy follows a certain probability density function cannot accurately reflect its real output.

The method of accurately describing the uncertainty of renewable energy power generation is the key to improving the ability of microgrids to deal with the uncertainty. In this condition, deep networks have certain application potential. Different from convolutional neural network [15], generative adversarial networks (GAN) can generate new data by alternating the training of generators and discriminators. For example, reference [16] uses GAN to generate renewable energy generation scenarios and proves that the GAN-based scenario generation method works well to restore the temporal correlation of renewable energy power generation. In reference [17–19], the scenario generation method based on GAN is applied to the optimization problem of power systems to improve the adaptability under the scenario of high permeability of renewable energy. Reference [20] first uses GAN to generate massive daily scenarios that can describe the uncertainty of renewable energy generation and then uses a clustering algorithm to improve the solving efficiency of optimal allocation of energy storage, obtain allocation results with stronger adaptability to the uncertain environment, and realize the maximum utilization efficiency of renewable energy in a grid-connected microgrid. The above references all use typical days as operation scenarios for power grid scheduling and allocation. However, with the increasing permeability of renewable energy within the microgrid, the high-dimensional nature of renewable energy power generation is becoming increasingly prominent, and the power output at the source end of the microgrid is difficult to describe in typical scenarios with daily cycles. Therefore, it is necessary to fully consider the renewable energy generation of each day and period in the longer dispatching cycle during the energy storage allocation stage of the microgrid.

In view of the high dimension of renewable energy generation, reference [21] integrates the multi-day energy scheduling strategy based on arbitrage-sensing linear programming into the process of energy storage capacity allocation of microgrids, reducing the cost of the whole life cycle of microgrids. Further, based on the Markov Chain Monte Carlo (MCMC) algorithm to generate a daily state transition process and combined with the day-day scenario generation method, reference [22] generates a multi-day net generation power scenario set covering landscape uncertainty on a long-time scale. It improves the economy of leasing capacity planning for microgrids. However, when MCMC is used to generate a daily state transfer process set, a large number of transfer processes need to be generated to reflect the real probability distribution of each daily state [23]. In the energy storage capacity allocation problem of microgrids, in order to improve the efficiency of solving subsequent stochastic optimization problems, in general, it is necessary to further use scenario reduction to obtain a typical scenario set containing a small number of scenario sets [24], which may lead to a large deviation between the occurrence frequency of each day state in the typical scenario set and the true probability, thus affecting the accuracy of the energy storage capacity optimization results of microgrid.

In order to comprehensively consider the high dimension and uncertainty of renewable energy generation, this paper proposes a microgrid energy storage capacity allocation method that takes into account the uncertainty of renewable energy generation: Firstly, by combining the intra-day scenario generation methods of LHS and Conditional Generative Adversarial Networks (CGAN), the typical multi-day scenario set is generated. Then, the obtained multi-day typical scenario set is used as a simulation operation scenario and input to the double-layer optimal allocation model of microgrid energy storage capacity, and finally, the optimal energy storage allocation strategy is obtained by using the PSO algorithm nested with the CPLEX solver. Compared with the existing research, the main work and innovation of this paper include:

(1) In order to solve the problem of energy storage capacity allocation of microgrids under the scenario of uncertain renewable energy generation, a double-layer optimization allocation model of energy storage capacity of microgrids is constructed by taking a multi-day typical scenario as the simulation operation scenario. The upper layer aims to optimize the energy storage allocation capacity by minimizing the expected annual total cost of centralized operation of the microgrid in multi-day typical scenarios, and the lower layer aims to optimize the microgrid operation plan under each typical scenario by minimizing the operation cost;

(2) In view of the uncertainty and high dimension of renewable energy generation, a scenario generation method combining CGAN and LHS with a long dispatching period was proposed. CGAN was used to excavate the output characteristics of renewable energy under each daily state type, and LHS was used to stratify sampling to avoid the large deviation between the occurrence frequency of each daily state and the true probability in the typical scenario set. At the same time, intra-day and inter-day scheduling of energy storage can be fully considered.

2. Energy Storage Capacity Allocation Model of Microgrid

As shown in Figure 1, the microgrid consists of microgas turbines, wind turbine units, photovoltaic units, user loads, and energy storage equipment. A common AC bus exists in the microgrid, connecting its different components, and they can be easily integrated into a conventional AC power system, providing more controllability and flexibility [25]. Among them, the energy storage equipment is connected to the common bus through AC-DC converters, which cause some energy loss during their charging and discharging processes [26,27].

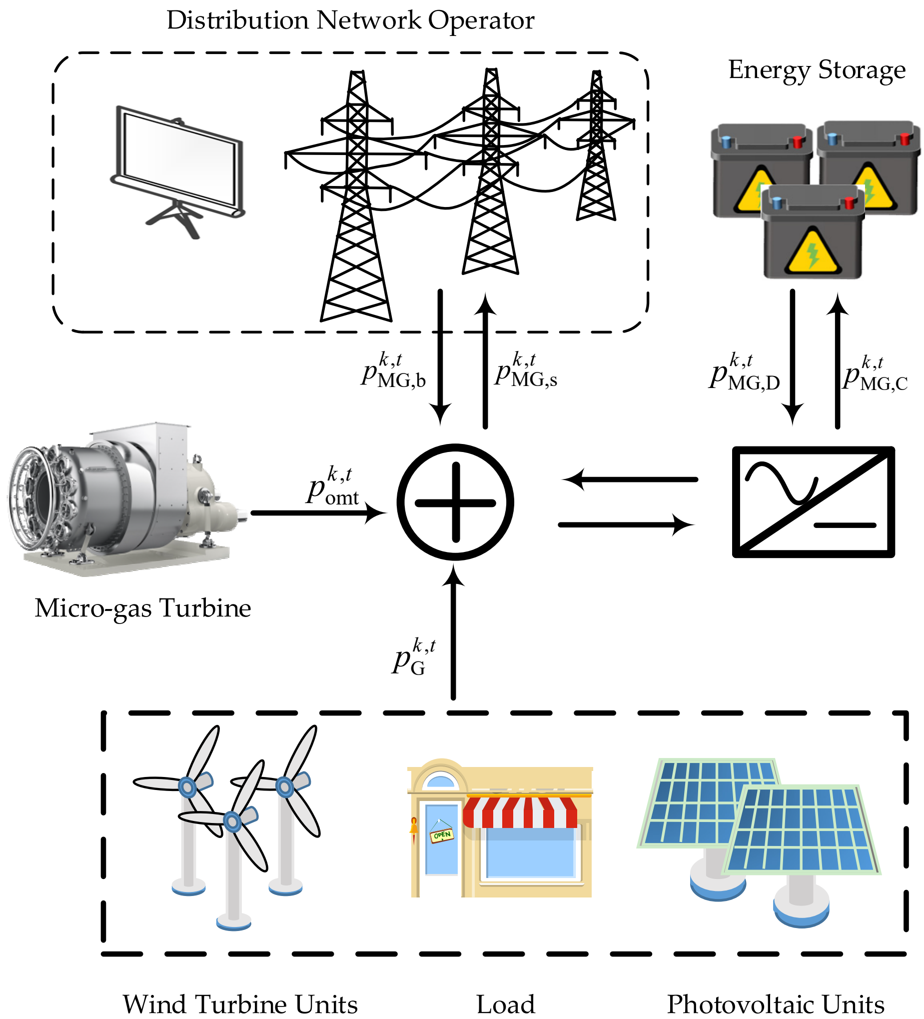

Figure 1. Structure of microgrid.

In the dispatching process, the microgrid gives priority to the use of renewable energy generation to meet its own load. The remaining net generation power is fed into the distribution network system after being stabilized by energy storage. If the net generation power is positive, it means that the residual power of the microgrid is transferred to the distribution network; if it is negative, it means that the power supply from the distribution network supports its own power balance [28].

2.1. Objective Function

The energy storage capacity allocation model of a microgrid consists of an upper layer and a lower layer. In the upper layer, the energy capacity and power capacity of the energy storage are configured with the minimum annual total cost C_{MG} of the microgrid as the target, and the objective function is:

$$\min C_{\mathrm{MG}} = C_{\mathrm{bess}} + 365 \times C_{\mathrm{po}} / N_{\mathrm{day}} \tag{1}$$

$$C_{\mathrm{bess}} = (\alpha \cdot Q_{\mathrm{E}} + \beta \cdot Q_{\mathrm{P}}) \frac{r(1+r)^{y}}{(1+r)^{y} - 1} \tag{2}$$

where C_{bess} is the annual cost of energy storage capacity investment; C_{po} is the operation cost expectation within the typical scenario set of a microgrid; N_{day} indicates the number of days in the typical scenario. In this paper, the value is 7. α and β are unit energy capacity and power capacity cost coefficient, respectively; r is the discount rate; y is energy storage life; Q_{E} and Q_{p} are, respectively, the energy storage capacity and power capacity configured for microgrid. Due to geographical and financial constraints, the maximum energy storage capacity that can be configured for microgrids is limited, so the value of Q_{E} in this paper is not more than 3000, and the value of Q_{p} is not more than 300.

On the lower level, the output plan of each piece of equipment in the microgrid is optimized with the goal of achieving a minimum operating cost expectation C_{po} within the typical scenario set of the microgrid, and its objective function is as follows:

$$\min C_{\mathrm{po}} = C_{\mathrm{bs}} + C_{\mathrm{yw}} + C_{\mathrm{bd}} + C_{\mathrm{omt}} \tag{3}$$

$$C_{\mathrm{bs}} = \sum_{k} \pi_k \sum_{t=1}^{T} (\rho_{\mathrm{s}}^{t} \cdot p_{\mathrm{MG,b}}^{k,t} - \rho_{\mathrm{b}}^{t} \cdot p_{\mathrm{MG,s}}^{k,t}) \tag{4}$$

$$C_{\mathrm{yw}} = \gamma \sum_{k} \pi_k \sum_{t=1}^{T} \left(p_{\mathrm{MG,C}}^{k,t} + p_{\mathrm{MG,D}}^{k,t} \right) \tag{5}$$

$$C_{\mathrm{bd}} = \varepsilon \sum_{k} \pi_k \sum_{t=1}^{T} (p_{\mathrm{MG,b}}^{k,t} - p_{\mathrm{MG,s}}^{k,t} - p_{\mathrm{ave}}^{k})^2 \tag{6}$$

$$p_{\mathrm{bs,ave}}^{k} = \sum_{t=1}^{T} (p_{\mathrm{MG,b}}^{k,t} - p_{\mathrm{MG,s}}^{k,t})/T \tag{7}$$

$$C_{\mathrm{omt}} = w \sum_{k} \pi_k \sum_{t=1}^{T} \left(p_{\mathrm{omt}}^{k,t} \right) \tag{8}$$

where, C_{bs} is the cost expectation of purchasing and selling electricity interactively with the distribution network; C_{yw} is the cost expectation of charging and discharging energy storage devices; C_{bd} is the penalty cost expectation of grid connected power fluctuation. C_{omt} is the fuel and pollutant emission cost expectation of the microgas turbine; w is the cost of fuel consumption per unit power output and pollutant emission treatment; $p_{\mathrm{omt}}^{k,t}$ is the output power of the micro-gas turbine at time t in typical scenario k, and its value is no less than zero. π_k is the probability of occurrence in scenario k; γ is unit charge and discharge cost coefficient; ρ_{b}^{t} and ρ_{s}^{t} respectively represent the purchasing and selling prices of the power distribution network in time period t; $p_{\mathrm{MG,b}}^{k,t}$ and $p_{\mathrm{MG,s}}^{k,t}$ are respectively the purchased and sold power of the microgrid at time t in typical scenario k, and their values are no less than zero. $p_{\mathrm{MG,C}}^{k,t}$ and $p_{\mathrm{MG,D}}^{k,t}$ are the charging and discharging power of the microgrid at the t time period in typical scenario k, and their values are no less than zero. ε is the penalty factor for power fluctuation on grid-connected connection lines [29,30]. $p_{\mathrm{bs,ave}}^{k}$ indicates the average power of grid-connected connection lines in a typical scenario k; T represents the number of scheduling time periods. In this paper, each time period is 1 h, and the scheduling period is one week; that is, T = 168.

2.2. Constraint Condition

Energy storage charging and discharging power constraints of microgrid:

$$\max\left(p_{\mathrm{MG,C}}^{k,t}, p_{\mathrm{MG,D}}^{k,t} \right) \leq Q_{\mathrm{P}} \tag{9}$$

$$p_{\mathrm{MG,C}}^{k,t} \cdot p_{\mathrm{MG,D}}^{k,t} = 0 \tag{10}$$

State of charge (SOC) constraints for energy storage of microgrid [31,32]:

$$0.1 \leq X_{\mathrm{MG,SOC}}^{k,t} \leq 0.9 \tag{11}$$

$$X_{\mathrm{MG,SOC}}^{k,t} = X_{\mathrm{MG,SOC}}^{k,t-1} + (p_{\mathrm{MG,C}}^{k,t} \cdot \eta + p_{\mathrm{MG,D}}^{k,t}/\eta) \cdot \Delta t / Q_{\mathrm{E}} \tag{12}$$

$$X_{\mathrm{MG,SOC}}^{k,T} = X_{\mathrm{MG,SOC}}^{k,0} \tag{13}$$

where $X_{\mathrm{MG,SOC}}^{k,t}$ is the SOC for energy storage at the end of time t in typical scenario k of microgrid; $X_{\mathrm{MG,SOC}}^{k,0}$ = 0.5 is the initial SOC for energy storage; Δt is the time period length; η is the charge and discharge efficiency of energy storage.

Power balance constraints of the microgrid:

$$p_{\mathrm{G}}^{k,t} + p_{\mathrm{MG,b}}^{k,t} + p_{\mathrm{MG,D}}^{k,t} - p_{\mathrm{MG,s}}^{k,t} - p_{\mathrm{MG,C}}^{k,t} - p_{\mathrm{loss}}^{k,t} = 0 \tag{14}$$

where $p_{\mathrm{G}}^{k,t}$ and $p_{\mathrm{loss}}^{k,t}$ respectively represent the net generation power and total wind and photovoltaic discard power of the microgrid at time t in typical scenario k, where the values are not less than zero.

Constraints on purchasing and selling power of the microgrid:

$$\max\left(p_{\mathrm{MG,b}}^{k,t}, p_{\mathrm{MG,s}}^{k,t}\right) \le p_{\mathrm{MG,bs}} \tag{15}$$

$$p_{\mathrm{MG,b}}^{k,t} \cdot p_{\mathrm{MG,s}}^{k,t} = 0 \tag{16}$$

Output power constraints of micro-gas turbines in the microgrid:

$$p_{\mathrm{omt}}^{k,t} \le p_{\mathrm{omt,max}}^{k,t} \tag{17}$$

$$\left|p_{\mathrm{omt}}^{k,t} - p_{\mathrm{omt}}^{k,t-1}\right| \le R \tag{18}$$

where, R is the climbing power limit of the microgas turbine.

3. Model Solving Process

3.1. Scenario Generation of Daily Net Generation Power Based on CGAN

The generation of the renewable energy unit of the microgrid gives priority to meeting its load demand, and then the remaining net generation power $p_{\mathrm{G}}^{k,t}$ is obtained as follows:

$$p_{\mathrm{G}}^{k,t} = p_{\mathrm{w}}^{k,t} + p_{\mathrm{pv}}^{k,t} - p_{\mathrm{load}}^{k,t} \tag{19}$$

where, $p_{\mathrm{w}}^{k,t}$, $p_{\mathrm{pv}}^{k,t}$ and $p_{\mathrm{load}}^{k,t}$ are respectively wind power, photovoltaic power, and load power of the microgrid at time t in a typical scenario k.

During the training of CGAN, daily state is taken as label c, and each historical net charge and discharge power scenario is labeled, and it is taken as the real training sample x, which is input into CGAN for training together with noise z, and output to generate scenario $x' = \mathrm{G}(z|c)$ through generating network G.

The discriminant network D of CGAN needs to measure the similarity between the generated scenario distribution $p(x')$ and the historical scenario distribution $p(x)$ according to Wasserstein distance and judge whether the generated scenario x' meets the corresponding label c. The objective function of CGAN training is:

$$\min_{G}\max_{D} V(\mathrm{D},\mathrm{G}) = E_{x\sim p(x)}[\mathrm{D}(x \mid c)] - E_{x'\sim p(x')}\left[\mathrm{D}\left(x' \mid c\right)\right] - \lambda E[\|\mathrm{D}(\ \sim)\| - 1]^2 \tag{20}$$

where E is the expected value of the corresponding distribution; λ is the regular term coefficient.

3.2. Scenario Generation of Multi-Day Net Generation Power

In order to determine the daily state of historical net generation power scenarios, DBI [33] was used to evaluate the optimal clustering number, and the K-means algorithm was used to cluster the scenarios in the historical scenario set into K types. According to the daily state and its frequency obtained by clustering, the probability density distribution P_r of daily state types can be calculated as follows:

$$P_r = [p_{\mathrm{r},1}\ p_{\mathrm{r},2}\ \ldots\ p_{\mathrm{r},K}] \tag{21}$$

$$p_{\mathrm{r},i} = \frac{n_i}{N} \tag{22}$$

where $p_{\mathrm{r},i}$ is the probability of the occurrence of daily state i (i = 1, 2..., K), N is the total number of days of historical data; n_i is the number of times state i occurs in the historical data.

The cumulative probability distribution $\boldsymbol{F}_\mathrm{r}$ of daily state types is further calculated as follows:

$$\boldsymbol{F}_\mathrm{r} = [f_0\ f_1\ f_2\ \ldots\ f_{K+1}] \tag{23}$$

where $f_i = \sum\limits_{j=1}^{i} p_{\mathrm{r},j}$ and $f_0 = 0$.

LHS divided the total sampling interval into several fixed cells and sampled only once in each cell, so as to ensure that no daily state scenario was ignored [34]. In this paper, M multi-day scenarios with N_{day} days were pre-constructed, then M times were sampled for a N_{day}-dimensional vector space, and 0-1 uniform sampling was carried out for each dimension. Each dimension in N_{day}-dimensional vector space was evenly divided into M intervals, and unified processing was carried out for N_{day}-dimensional vector space. First, all subintervals are traversed, N_{day} values are randomly selected from the ith subinterval to form the ith column of the matrix $\boldsymbol{A}$, and the matrix $\boldsymbol{A}$ is finally obtained as follows:

$$\boldsymbol{A} = \begin{bmatrix} p_{11} & p_{12} & \cdots & p_{1M} \\ p_{21} & p_{22} & \cdots & p_{2M} \\ \vdots & \vdots & & \vdots \\ p_{N_{day}1} & p_{N_{day}2} & \cdots & p_{N_{day}M} \end{bmatrix} \tag{24}$$

Then, leave the order of columns $\boldsymbol{A}$ unchanged and randomly shuffle the order of each row to obtain the matrix $\boldsymbol{B}$. Next, according to each element $p_{i,j}$ in matrix $\boldsymbol{B}$, the daily state scenario set matrix $\boldsymbol{D}$ is obtained as follows:

$$\boldsymbol{D} = \begin{bmatrix} D_{11} & D_{12} & \cdots & D_{1M} \\ D_{21} & D_{22} & \cdots & D_{2M} \\ \vdots & \vdots & & \vdots \\ D_{N_{day}1} & D_{N_{day}2} & \cdots & D_{N_{day}M} \end{bmatrix} \tag{25}$$

where $D_{ij} = k$, $(f_{k-1} \leq p_{ij} < f_k)$, and D_{ij} is the state type of the daily scenario, and each column of matrix $\boldsymbol{D}$ represents a multi-day scenario state transition process containing N_{day} days.

Finally, as shown in Figure 2, each element of $\boldsymbol{D}$ matrix is taken as label c and noise z is taken as driver, which is input into the trained CGAN model to generate the corresponding intra-day scenarios, and then the scenario sets of multiple multi-day net generation power scenarios are obtained according to the label sequence.

3.3. Multi-Day Scenario Reduction

Scenario reduction improves the efficiency of solving stochastic optimization problems but also causes the loss of uncertainty information about renewable energy generation, which will affect the results of stochastic optimization. To retain the information that affects the result to the maximum extent, three features, namely average power p^i_{ave}, power mean square error p^i_σ, and peak-valley difference $p^i_{\mathrm{M-m}}$, are selected as the attributes of scenario i. Among them, the average power reflects the surplus and deficiency degrees of net generating power in the dispatching cycle of the microgrid, and the peak-valley difference reflects the demand of the microgrid for "peak shaving and valley filling", and then reflects the demand of the microgrid for energy storage. Power mean square error directly affects the power fluctuation penalty cost of microgrids and then affects the result of energy storage allocation capacity. The calculation formula for the above three features is as follows:

$$p^i_{\text{ave}} = \sum_{t=1}^{T} \left(P^i_{\text{G},t} \right) / T \tag{26}$$

$$p^i_{\sigma} = \sum_{t=1}^{T} \left(P^i_{\text{G},t} \right)^2 / T \tag{27}$$

$$p^i_{\text{M-m}} = \max_{1 \le t \le T} \left(P^i_{\text{G},t} \right) - \min_{1 \le t \le T} \left(P^i_{\text{G},t} \right) \tag{28}$$

where $P^i_{\text{G},t}$ is the net generating power at time t in scenario i. In this paper, each time period is 1 h, and the scheduling period is one week; that is, T = 168. Then, the K-means algorithm is used to reduce the scenarios. The distance between the ith scenario X_i and the jth scenario X_j is calculated as follows:

$$d_{ij} = \sqrt{\begin{array}{l} \left(\text{norm}(p^i_{\text{ave}}) - \text{norm}(p^j_{\text{ave}})\right)^2 + \\ \left(\text{norm}(p^i_{\sigma}) - \text{norm}(p^j_{\sigma})\right)^2 + \\ \left(\text{norm}(p^i_{\text{M-m}}) - \text{norm}(p^j_{\text{M-m}})\right)^2 \end{array}} \tag{29}$$

where $\text{norm}(y^i)$ is the calculation normalized to [0, 1], and its formula is as follows:

$$\text{norm}(y^i) = \frac{y^i - \min\limits_{1 \le i \le N_s} y^i}{\max\limits_{1 \le i \le N_s} y^i - \min\limits_{1 \le i \le N_s} y^i} \tag{30}$$

where N_{s} is the number of scenarios in the scenario set; y^i can be the average power p^i_{ave}, the power mean square error p^i_{σ} and the peak-valley difference $p^i_{\text{M-m}}$.

After the clustering algorithm is used to reduce, the probability of the occurrence of the kth typical scenario π_k is calculated as follows:

$$\pi_k = \frac{N_k}{M} \tag{31}$$

where N_k is the number of scenarios belonging to the k class.

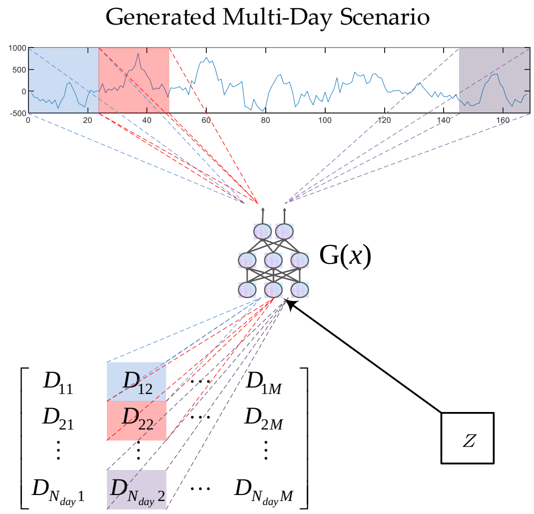

Figure 2. Generation of multi-day net power generation scenarios.

3.4. Double-Layer Optimal Allocation Model Solving

The optimal allocation model of the energy storage capacity of a microgrid can be divided into upper and lower layers. The approach of using a heuristic algorithm as a nested solver can solve the double-layer optimization model efficiently [35–38]. The upper layer uses the PSO algorithm to search for the optimal capacity of energy storage (power capacity, energy capacity) and sends the capacity information as a constraint to the lower random optimization model. The lower layer uses the CPLEX solver to solve the output plan of the dispatchable equipment in each typical scenario of the microgrid at each time period and transmits the expectation of operation cost back to the upper layer. The scenario set of net discharge power used for the lower-level operation optimization is generated using the method proposed in Section 2. The specific process is shown in Figure 3.

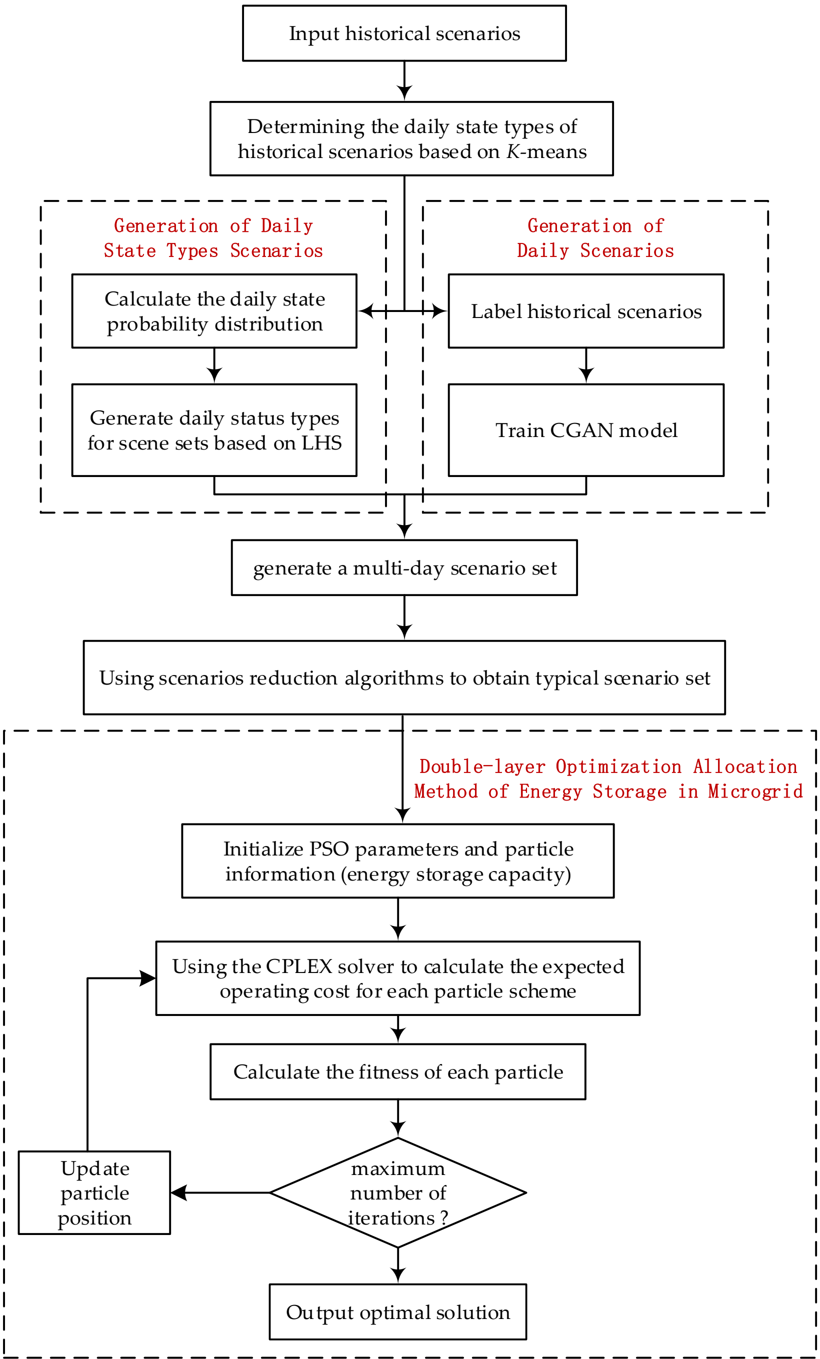

Figure 3. Model-solving process.

4. Example Analysis

4.1. Example Parameter

This paper adopts the one-year actual data of wind power, photovoltaic power, and load power of a microgrid in a region of our country as the historical scenario data set and sets the sampling interval to 1 h. CGAN is constructed by the TensorFlow framework, and the specific setting of network parameters is referred to in reference [16]. The parameters of the microgrid are set as shown in Table A1.

4.2. Simulation Results and Analysis

4.2.1. Comparison of Generation Methods for Typical Scenarios of Net Generating Power

In order to verify the superiority of the generation method of the typical scenario set of net power generation proposed in this paper, 20 daily state transition processes were generated based on MCMC and LHS, respectively, and typical scenario sets with different numbers of scenarios were obtained. Then, the occurrence frequency of each daily state in the generation of the typical scenario set was counted, and the expected probability $p_{\mathrm{E},i}$ of the occurrence of daily state i was further calculated.

$$p_{\mathrm{E},i} = \sum_{k} \pi_k p_{\mathrm{f},i}^{k} \tag{32}$$

where $p_{\mathrm{f},i}^{k}$ is the occurrence frequency of state k in scenario i.

The results are shown in Tables 1 and 2, in which the true occurrence probabilities of each daily state obtained according to historical data are 26.24%, 37.43%, and 36.33%, respectively. As can be seen from Tables 1 and 2, when the number of reserved scenarios in the typical scenario set is small, the probability expectation of each day state obtained based on the MCMC method has a significant deviation from the real probability, while the probability expectation of each day state obtained based on the LHS method has little difference. This is because LHS, as a stratified sampling algorithm, can ensure that the sampling rate between each cell can be taken into account even when the sampling times are small. Therefore, it shows that the generation method of the typical scenario set of net power generation proposed in this paper can still guarantee the probability expectation of the occurrence of each daily state and avoid ignoring individual daily state scenarios even when the number of scenarios in the typical scenario set is small.

Table 1. Probability expectations of daily state obtained by the MCMC method under different number of reserved scenarios.

Number of Reserved Scenarios	Expected Probability/%		
	Daily State 1	Daily State 2	Daily State 3
3	42.85	33.33	23.81
5	34.28	42.86	22.85
10	28.57	38.57	32.56

Table 2. Probability expectations of daily state obtained by the LHS method under different number of reserved scenarios.

Number of Reserved Scenarios	Expected Probability/%		
	Daily State 1	Daily State 2	Daily State 3
3	28.57	38.10	33.33
5	28.57	34.29	37.14
10	25.71	38.57	35.71

4.2.2. Energy Storage Capacity Optimization Allocation Results and Analysis

Taking $M = 20$ and $K = 3$, the typical scenario set after scenario reduction and its autocorrelation coefficient are shown in Figure 4, where the probability of each multi-day typical scenario is 25%, 40%, and 35%, respectively. In Figure 4, the top row is a comparison of the typical scenario set and the scenario set. The bottom row is the autocorrelation coefficient of the scenario. As can be seen from the upper row of Figure 4, the typical scenario set can reflect the ups and downs of the scenario set and better depict the uncertainty of new renewable energy power generation. As can be seen from the lower row of Figure 4, the typical scenario well preserves the time correlation of the original scenario because CGAN can well capture the time correlation of the renewable energy output curve.

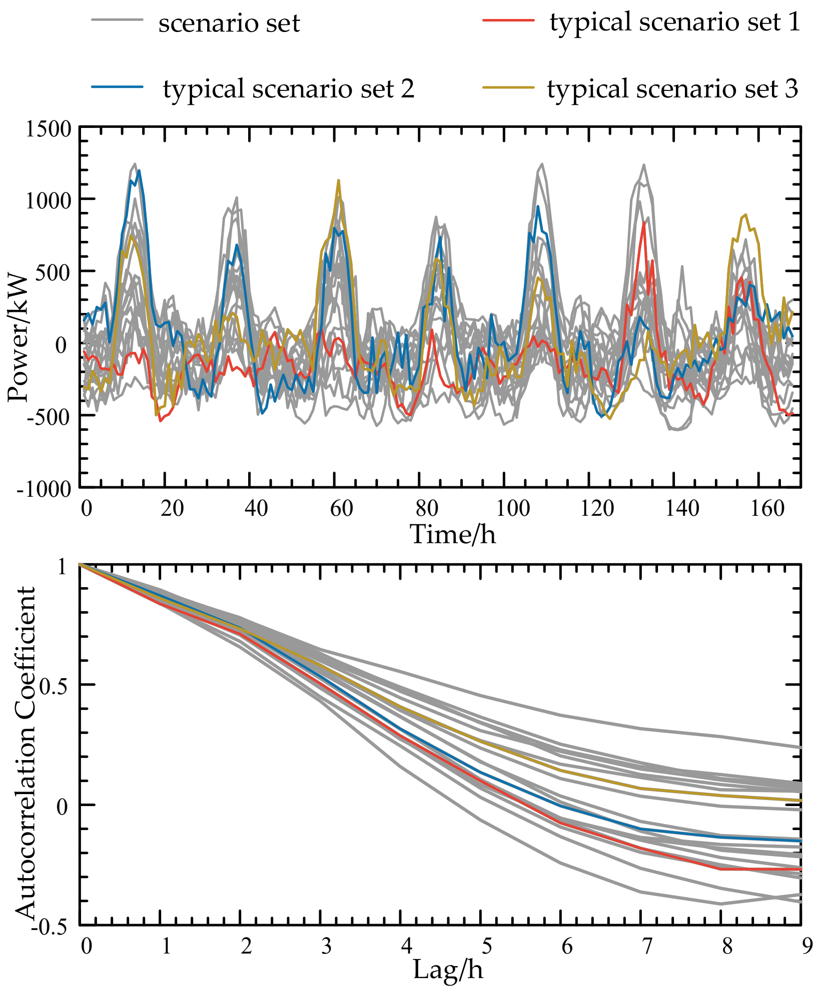

Figure 4. Collection of typical scenarios.

Figure 5 shows the iterative process of the particle swarm optimization algorithm. Both the population size and the maximum number of iterations are set to 20; the inertia weight is set to 0.5; and the learning factors for individuals and society are set to 0.4 and 0.6, respectively. As can be seen from the figure, the algorithm converges quickly to the optimal solution, i.e., it converges to the optimal fitness of −115,074.7 in the 8th generation. This is because the solution dimension of the upper layer optimal energy storage lease price problem is small (only energy capacity price and power capacity price), so the use of the PSO algorithm with easily set parameters is sufficient for the model solution. The final optimal energy capacity of the microgrid energy storage is 1804.5 kWh, the optimal energy capacity is 269.0 kW, and the total expected annual cost of the microgrid is CNY 115,074.7.

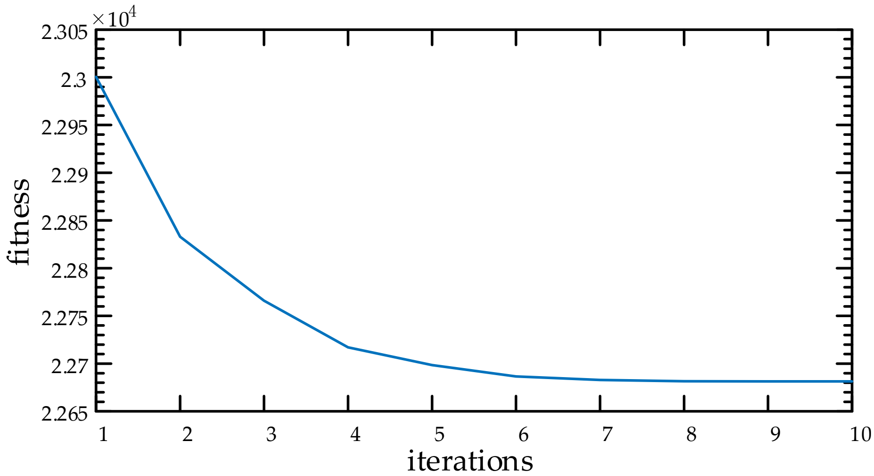

Figure 5. Iterative process.

The variation of the mean square error of contact line power before and after microgrid suppression in each typical scenario is shown in Table 3 As can be seen from the table, after the microgrid containing energy storage is suppressed, the mean square error of the power of the contact line between the microgrid and the distribution network decreases to a certain extent, which relieves the grid-connection pressure of renewable energy.

Table 3. The effect of the microgrid on suppressing fluctuations in each typical scenario.

	Mean Square Error of Contact Line Power/kW^2	
	Before Microgrid Suppression	**After Microgrid Suppression**
Typical Scenario 1	46,276	13,066
Typical Scenario 2	137,515	26,424
Typical Scenario 3	121,507	27,816

The planned output of equipment and changes in energy storage charge state in each period of typical multi-day scenarios are shown in Figure 6, where the first to third rows correspond to the operation plans of the first to third typical scenarios, respectively.

In Figure 6, the first column graph shows the equipment output plan at each period of typical scenarios: The purchase and sale of electricity in the microgrid represented by the purple bar reflect its grid-connection pressure. The energy storage discharge power represented by the upward blue bar exceeds the net load curve (the inverse of the net generating power), indicating that the energy storage discharge is sold to the distribution network; that is, the "discharging at peak" operation is implemented. The charging power of the energy storage, represented by the downward blue bar, exceeds the net load curve, indicating that the energy storage buys electricity from the distribution network and stores it; that is, the "charging at off-peak" operation is implemented. If the energy storage charging power does not reach the net load power, it means that the microgrid implements a wind abandonment operation. If the output of the micro-gas turbine represented by the orange bar exceeds the net load, it means that the power of the micro-gas turbine is sold to the distribution network. The second column graph shows the SOC of energy storage in corresponding typical scenarios, where the change in SOC of energy storage at the final moment of each day reflects the transfer of energy during the day. From the figure, we can see that the microgrid plays the role of "Peak Load Shifting" in each typical scenario, relieving the distribution grid's peak regulation pressure and gaining more profit through "charging at off-peak and discharging at peak". On the remaining power days, the microgrid tends to absorb more power to cope with the possible subsequent power shortage days, which not only relieves the pressure of new energy consumption on the remaining power days but also reduces the power purchased by the microgrid from the distribution grid on the shortage days and lowers its power consumption cost. Taking typical scenario 2 as an example, on the first day of surplus wind power and photovoltaic power, the microgrid sells electricity to the distribution network for profit. At the same time, the energy storage absorbs part of the surplus power to prepare for possible power shortage days in the future and abandons the peak part of wind power and photovoltaic power. On the second day, when wind power and photovoltaic power were insufficient, the microgrid not only used energy storage discharge to meet its own load demand but also sold part of the electric energy to the distribution network to assist it in peak regulation and make profits. Finally, the interactive power fluctuation of the link line significantly decreased compared with the net load power fluctuation before leveling off. To sum up, energy storage planning of microgrids based on typical scenarios of multi-day net generation power can obtain a more reasonable energy storage capacity allocation by comprehensively considering the day-to-day energy transfer demand of the microgrid while reducing the fluctuation of grid-connected net generation power and alleviating the consumption pressure of renewable energy.

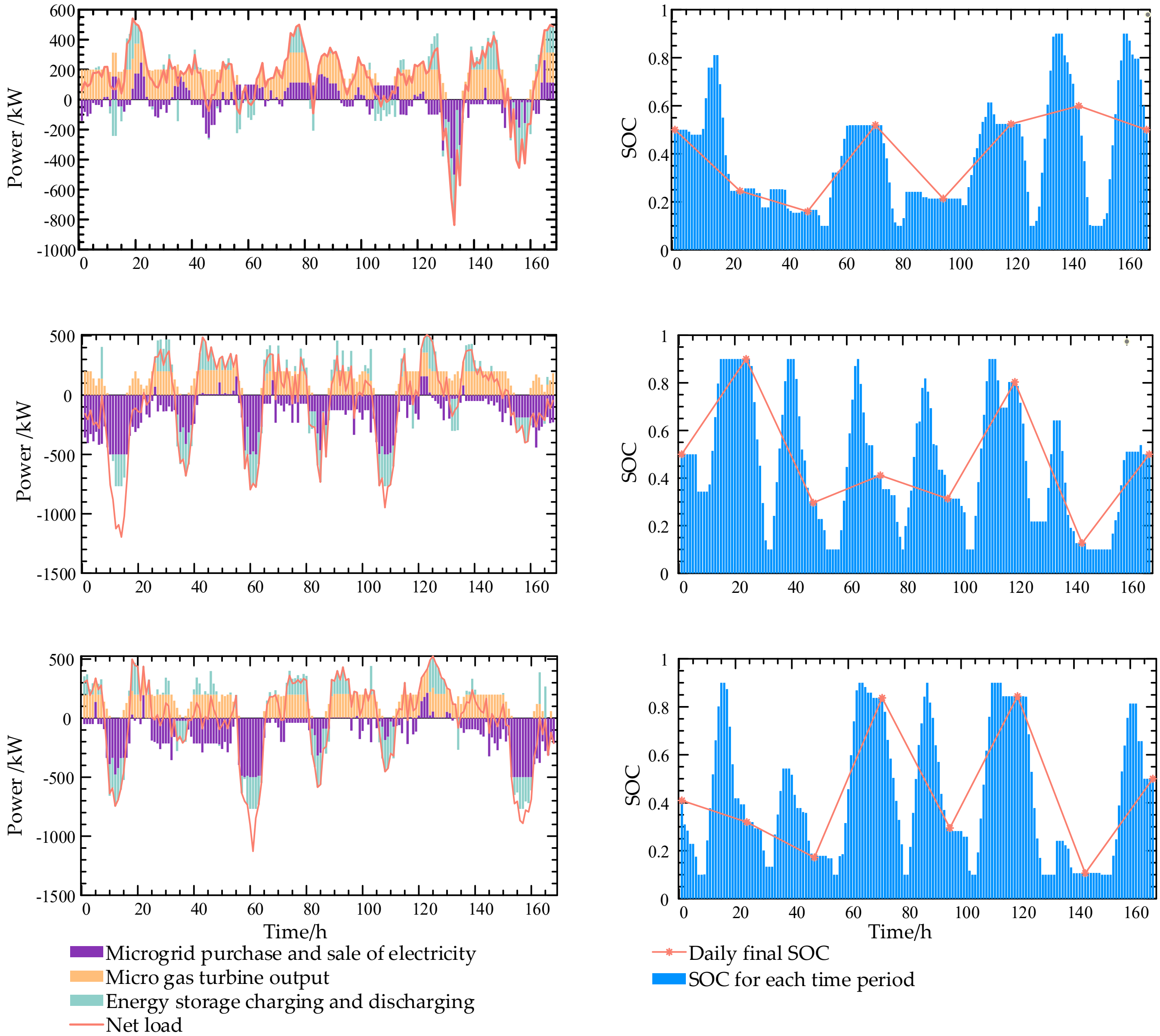

Figure 6. Operation plan of each scenario.

4.2.3. The Ability of Microgrids to Cope with The Uncertainty of Renewable Energy Generation under Different Algorithms

In order to prove the adaptability of the energy storage capacity optimization allocation method proposed in this paper to the uncertain environment of renewable energy generation, the optimization results of several energy storage capacity allocation methods were compared and analyzed, and 20 real scenarios with a duration of one week were randomly selected as test scenarios. In the test scenario, the operation economy of microgrids under different planning results and the ability to suppress the power fluctuation of renewable energy were compared.

Method 1: The method of stochastic optimal allocation of energy storage capacity in reference [14] was adopted.

Method 2: The optimization method based on typical days in reference [18] was adopted, that is, the GAN scenario generation method was used to generate massive daily scenarios, and then the clustering algorithm was used to reduce massive daily scenarios to obtain typical scenarios, and typical scenarios were used as simulation operation scenarios to optimize energy storage capacity.

Method 3: Use the energy storage optimization allocation method based on the typical multi-day scenarios proposed in this paper.

The energy storage capacity optimization results of different methods, the average grid-connected power of the microgrid in the test scenario, and the average total annual cost of the test scenario are shown in Table 4.

Table 4. Comparison of the results of different methods.

	E_{cap} /kWh	P_{cap} /kW	Average of Mean Square Error of Contact Line Power/kW^2	Wind and Photovoltaic Abandonment Power/kWh	Average Annual Total Cost
Method 1	1168.9	217.4	2,181,846.5	110,091.6	CNY 574,050.4
Method 2	1546.4	250.0	1,896,224.6	86,019.2	CNY 513,249.3
Method 3	1804.5	269.0	1,736,419.9	72,973.4	CNY 479,736.0

Compared with Method 1, Method 2 is equipped with more energy storage capacity, has a better power fluctuation suppression effect, reduces wind and photovoltaic abandonment power by 21.87%, and reduces the average annual total cost of microgrid operation by 11.85% in the test scenario. This is because, compared with the method that assumes that the generation of wind power and photovoltaic power conforms to the specific probability density distribution, the scenario generation method based on GAN can not only reflect the probability density distribution of the generation of renewable energy more accurately but also make the generation scenario have a better time correlation. Thus, the generation scenario of Method 2 can better describe the uncertainty of renewable energy generation, so as to make the microgrid have better economy in the test scenario. Compared with Method 1 and Method 2, the average annual total cost of Method 3, which has the largest energy storage capacity, decreases by 19.66% and 6.99%, respectively, and the wind and photovoltaic abandonment power decreases by 33.72% and 15.17%, respectively. While reducing the annual total cost, it further improves the ability of the microgrid to suppress power fluctuations. This is because, compared with the typical day scenario adopted in Method 2, the multi-day typical scenario adopted in Method 3 takes into account the high dimension of renewable energy generation, so more energy storage capacity is configured to meet the energy scheduling requirements of surplus days and absence days. At the same time, the multi-day scenario can better describe the uncertainty of renewable energy in each day and time period than the daily scenario, which further improves the renewable energy absorption capacity and adaptability of the microgrid to the uncertainty of renewable energy.

5. Conclusions

In order to cope with the uncertainty of renewable energy generation at a long-time scale and relieve the grid-connected pressure of net generation power in microgrids, a microgrid energy storage capacity allocation method was proposed, taking into account the uncertainty of renewable energy generation. Typical scenario sets of multi-day net generation power were used to depict the uncertainty of renewable energy generation and optimize the allocation of energy storage capacity in microgrids. An example analysis verifies the proposed model and draws the following conclusions:

(1) In the process of energy storage capacity allocation in microgrids, the proposed double-layer optimal allocation model of energy storage capacity in microgrids comprehensively considers the influence of daytime and intra-day scheduling strategies on the allocation problem, which ensures the operation economy and relieves the grid-connected pressure of net generation power;

(2) The generation method of typical scenarios of multi-day net generation power proposed can still restore the real situation of daily state probability density distribution when the number of typical scenarios is small. The time correlation and uncertainty of renewable energy generation are explored by using CGAN to avoid the assumption that renewable energy generation obeys a certain probability distribution.

The uncertainty of cold and heat loads in the microgrid is not considered in this paper. In future studies, detailed modeling will be carried out for the microgrid containing the integrated energy system of electricity, gas, heat, and cold, so as to better relieve the renewable energy consumption pressure of the microgrid and further improve its ability to deal with the uncertainty of source load.

Author Contributions: Conceptualization, W.W. and L.Y.; methodology, W.W. and Y.F.; software, Y.W. and X.C.; validation, Y.W. and X.C.; resources, Z.L.; writing—original draft preparation, X.C.; writing—review and editing, Z.L. All authors have read and agreed to the published version of the manuscript.

Funding: This work was funded by the National Natural Science Foundation of China (NSFC) by the Chinese government (grant nos. 52277012), and the Science and Technology Program of State Grid Hubei Electric Power Co., Ltd. (B31543220914).

Institutional Review Board Statement: Not applicable.

Informed Consent Statement: Not applicable.

Data Availability Statement: Not applicable.

Conflicts of Interest: The authors declare no conflict of interest.

Appendix A

Table A1. Microgrid parameter setting.

Parameter	Value
α	CNY 1000 per kWh
β	CNY 3500 per kW
r	0.067
y	10 years
R	500 kW
γ	CNY 0.1542 per kWh
ε	0.15
w	CNY 0.142 per kWh
η	95%
$p_{\mathrm{MG,bs}}$	500 kW

References

1. Wang, R.; Li, C.; Fu, W.; Tang, G. Deep Learning Method Based on Gated Recurrent Unit and Variational Mode Decomposition for Short-Term Wind Power Interval Prediction. *IEEE Trans. Neural Netw. Learn. Syst.* **2020**, *31*, 3814–3827. [CrossRef] [PubMed]
2. Fang, P.; Fu, W.; Wang, K.; Xiong, D.; Zhang, K. A compositive architecture coupling outlier correction, EWT, nonlinear Volterra multi-model fusion with multi-objective optimization for short-term wind speed forecasting. *Appl. Energy* **2022**, *307*, 118191. [CrossRef]
3. Huang, B.; Li, Y.; Zhang, H.; Sun, Q. Distributed optimal co-multi-microgrids energy management for energy internet. *IEEE/CAA J. Autom. Sin.* **2016**, *3*, 357–364.
4. Zhang, Y.; Wei, L.; Fu, W.; Chen, X.; Hu, S. Secondary frequency control strategy considering DoS attacks for MTDC system. *Electr. Power Syst. Res.* **2023**, *214*, 108888. [CrossRef]
5. Zhang, Y.; Xie, X.; Fu, W.; Chen, X.; Hu, S.; Zhang, L.; Xia, Y. An Optimal Combining Attack Strategy Against Economic Dispatch of Integrated Energy System. *IEEE Trans. Circuits Syst. II Express Briefs* **2023**, *70*, 246–250. [CrossRef]
6. Xu, P.; Fu, W.; Lu, Q.; Zhang, S.; Wang, R.; Meng, J. Stability analysis of hydro-turbine governing system with sloping ceiling tailrace tunnel and upstream surge tank considering nonlinear hydro-turbine characteristics. *Renew. Energy* **2023**, *210*, 556–574. [CrossRef]
7. Nazir, M.S.; Abdalla, A.N.; Wang, Y.; Chu, Z.; Jie, J.; Tian, P.; Jiang, M.; Khan, I.; Sanjeevikumar, P.; Tang, Y. Optimization configuration of energy storage capacity based on the microgrid reliable output power. *J. Energy Storage* **2020**, *32*, 101866. [CrossRef]
8. El-Ela, A.A.A.; El-Seheimy, R.A.; Shaheen, A.M.; Wahbi, W.A.; Mouwafi, M.T. PV and battery energy storage integration in distribution networks using equilibrium algorithm. *J. Energy Storage* **2021**, *42*, 103041. [CrossRef]
9. El-Ela, A.A.A.; El-Sehiemy, R.A.; Shaheen, A.M.; Wahbi, W.A.; Mouwafi, M.T. A multi-objective equilibrium optimization for optimal allocation of batteries in distribution systems with lifetime maximization. *J. Energy Storage* **2022**, *55*, 105795. [CrossRef]
10. Guo, Y.; Zhao, C. Islanding-aware robust energy management for microgrids. *IEEE Trans. Smart Grid* **2016**, *9*, 1301–1309. [CrossRef]
11. Bozorgavari, S.A.; Aghaei, J.; Pirouzi, S.; Nikoobakht, A.; Farahmand, H.; Korpås, M. Robust planning of distributed battery energy storage systems in flexible smart distribution networks: A comprehensive study. *Renew. Sustain. Energy Rev.* **2020**, *123*, 109739. [CrossRef]
12. Zhou, Y.; Zhai, Q.; Yuan, W.; Wu, J. Capacity expansion planning for wind power and energy storage considering hourly robust transmission constrained unit commitment. *Appl. Energy* **2021**, *302*, 117570. [CrossRef]
13. Li, K.; Zhang, J.; Che, J.; Wang, F.; Ren, H.; Mi, Z. Capacity configuration optimization for stand-alone microgrid considering the uncertainties of wind and solar resource. In Proceedings of the 2018 IEEE Power & Energy Society Innovative Smart Grid Technologies Conference (ISGT), Washington, DC, USA, 21–25 October 2018; pp. 1–5.
14. Atia, R.; Yamada, N. Sizing and analysis of renewable energy and battery systems in residential microgrids. *IEEE Trans. Smart Grid* **2016**, *7*, 1204–1213. [CrossRef]
15. Fu, W.; Jiang, X.; Li, B.; Tan, C.; Chen, B.; Chen, X. Rolling bearing fault diagnosis based on 2D time-frequency images and data augmentation technique. *Meas. Sci. Technol.* **2023**, *34*, 045005. [CrossRef]
16. Chen, Y.; Wang, Y.; Kirschen, D.; Zhang, B. Model-free renewable scenario generation using generative adversarial networks. *IEEE Trans. Power Syst.* **2018**, *33*, 3265–3275. [CrossRef]
17. Kong, X.; Xiao, J.; Liu, D.; Wu, J.; Wang, C.; Shen, Y. Robust stochastic optimal dispatching method of multi-energy virtual power plant considering multiple uncertainties. *Appl. Energy* **2020**, *279*, 115707. [CrossRef]
18. Li, Y.; Wang, B.; Yang, Z.; Li, J.; Chen, C. Hierarchical stochastic scheduling of multi-community integrated energy systems in uncertain environments via Stackelberg game. *Appl. Energy* **2022**, *308*, 118392. [CrossRef]
19. Li, Y.; Han, M.; Shahidehpour, M.; Li, J.; Long, C. Data-driven distributionally robust scheduling of community integrated energy systems with uncertain renewable generations considering integrated demand response. *Appl. Energy* **2023**, *335*, 120749. [CrossRef]
20. Chen, X.; Dong, W.; Yang, Q. Robust optimal capacity planning of grid-connected microgrid considering energy management under multi-dimensional uncertainties. *Appl. Energy* **2022**, *323*, 119642. [CrossRef]
21. Mohseni, S.; Brent, A.C. A Metaheuristic-Based Micro-Grid Sizing Model with Integrated Arbitrage-Aware Multi-Day Battery Dispatching. *Sustainability* **2022**, *14*, 12941. [CrossRef]
22. Chen, X.; Fu, W.; Zhang, H.; Zhang, Y.; Wang, R.; Li, J. Optimal Dispatching Strategy of Shared Energy Storage and Multi-Microgrid Considering the Uncertainty of New Energy Generation. *Power Syst. Technol.* **2023**, 1–17. (In Chinese)
23. Li, D.; Yan, W.; Li, W.; Ren, Z. A two-tier wind power time series model considering day-to-day weather transition and intraday wind power fluctuations. *IEEE Trans. Power Syst.* **2016**, *31*, 4330–4339. [CrossRef]
24. Heitsch, H.; Römisch, W. Scenario Reduction Algorithms in Stochastic Programming. *Comput. Optim. Appl.* **2003**, *24*, 187–206. [CrossRef]
25. Abbasi, M.; Abbasi, E.; Li, L.; Aguilera, R.P.; Lu, D.; Wang, F. Review on the Microgrid Concept, Structures, Components, Communication Systems, and Control Methods. *Energies* **2023**, *16*, 484. [CrossRef]
26. Pamulapati, T.; Cavus, M.; Odigwe, I.; Allahham, A.; Walker, S.; Giaouris, D. A Review of Microgrid Energy Management Strategies from the Energy Trilemma Perspective. *Energies* **2022**, *16*, 289. [CrossRef]

27. El-Ela, A.A.A.; El-Sehiemy, R.A.; Allam, S.M.; Shaheen, A.M.; Nagem, N.A.; Sharaf, A.M. Renewable Energy Micro-Grid Interfacing: Economic and Environmental Issues. *Electronics* **2022**, *11*, 815. [CrossRef]
28. Li, X.S.; Fang, Z.; Li, F.; Xie, S.; Cheng, S. Game-based Optimal Dispatching Strategy for Distribution Network with Multiple Microgrids Leasing Shared Energy Storage. *Proc. CESS* **2022**, *42*, 6611–6625. (In Chinese)
29. Li, S.; Zhu, J.; Dong, H.; Zhu, H.; Fan, J. A novel rolling optimization strategy considering grid-connected power fluctuations smoothing for renewable energy microgrids. *Appl. Energy* **2022**, *309*, 118441. [CrossRef]
30. Yang, N.; Qin, T.; Wu, L.; Huang, Y.; Huang, Y.; Xing, C.; Zhang, L.; Zhu, B. A multi-agent game based joint planning approach for electricity-gas integrated energy systems considering wind power uncertainty. *Electr. Power Syst. Res.* **2021**, *204*, 107673. [CrossRef]
31. Hamida, M.A.; El-Sehiemy, R.A.; Ginidi, A.R.; Elattar, E.; Shaheen, A.M. Parameter identification and state of charge estimation of Li-Ion batteries used in electric vehicles using artificial hummingbird optimizer. *J. Energy Storage* **2022**, *51*, 104535. [CrossRef]
32. El-Sehiemy, R.; Hamida, M.A.; Elattar, E.; Shaheen, A.; Ginidi, A. Nonlinear Dynamic Model for Parameter Estimation of Li-Ion Batteries Using Supply–Demand Algorithm. *Energies* **2022**, *15*, 4556. [CrossRef]
33. Tang, R.; Dore, J.; Ma, J.; Leong, P.H. Interpolating high granularity solar generation and load consumption data using super resolution generative adversarial network. *Appl. Energy* **2021**, *299*, 117297. [CrossRef]
34. Ma, Z.; Gao, J.; Hu, W.; Dinavahi, V. Risk-adjustable stochastic schedule based on Sobol augmented Latin hypercube sampling considering correlation of wind power uncertainties. *IET Renew. Power Gener.* **2021**, *15*, 2356–2367. [CrossRef]
35. Yang, N.; Dong, Z.; Wu, L.; Zhang, L.; Shen, X.; Chen, D.; Zhu, B.; Liu, Y. A Comprehensive Review of Security-constrained Unit Commitment. *J. Mod. Power Syst. Clean Energy* **2022**, *10*, 562–576. [CrossRef]
36. Yang, N.; Ye, D.; Zhou, Z.; Cui, J.; Chen, D.; Wang, X. Research on Modelling and Solution of Stochastic SCUC under AC Power Flow Constraints. *IET Gener. Transm. Distrib.* **2018**, *12*, 3618–3625.
37. Yang, N.; Yang, C.; Wu, L.; Shen, X.; Jia, J.; Li, Z.; Chen, D.; Zhu, B.; Liu, S. Intelligent Data-Driven Decision-Making Method for Dynamic Multisequence: An E-Seq2Seq-Based SCUC Expert System. *IEEE Trans. Ind. Inform.* **2022**, *18*, 3126–3137. [CrossRef]
38. Yang, N.; Yang, C.; Xing, C.; Ye, D.; Jia, J.; Chen, D.; Shen, X.; Huang, Y.; Zhang, L.; Zhu, B. Deep learning-based SCUC decision-making: An intelligent data-driven approach with self-learning capabilities. *IET Gener. Transm. Distrib.* **2022**, *16*, 629–640. [CrossRef]